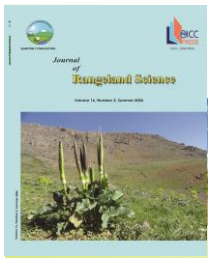

J. Rangeland Sci., 2026; 16(3): 278-288

Journal of Rangeland Science (JRS)

https://doi.org/10.57647/JRS.2026.1603.25

Research Article

Assessment of Integrated Landsat-8 and Sentinel-2 Images on Identification and Resolution of the Burned Rangelands (Case Study: Semi-steppe Rangelands in Chahar-Mahal Bakhtiari, Province, Iran)

Ali Mohammadian[1,*], Esmaeil Asadi Borojeni[2], Reza SiahMansour[1]

[1] *Lorestan Agricultural and Natural Resources Research and Education Center, Agricultural Research, Education and Extension Organization (AREEO), Khorramabad, Iran*

[2] *Natural Resources and Earth Sciences College, Shahrekord University, Shahrekord, Iran*

*Corresponding author: Mohammadian5392@gmail.com

Article History:

Received:
26 March 2025

Revised:
20 November 2025

Accepted:
19 December 2025

Published in Issue:
30 September 2026

©2026 the Author(s). Published by the OICC Press under the terms of the © CC BY 4.0, Creative Commons Attribution License, which permits use, distribution and reproduction in any medium, provided the original work is properly cited.

Abstract

Accurate monitoring of the combined impacts of fire and grazing on plant communities in semi-steppe rangelands is challenging due to spatial and temporal variability. This study demonstrates that integrating multi-sensor remote sensing data can significantly enhance monitoring precision.The Gram-Schmidt algorithm was employed to fuse Landsat-8 and Sentinel-2 imagery, improving spatial resolution from 30m to 10m while preserving spectral characteristics. In addition, pan-sharpening techniques enhanced Landsat-8 imagery to 15 m resolution. Classification of affected areas was performed using Maximum Likelihood Classification (MLC) with a comprehensive dataset including spectral bands, the Normalized Burn Ratio Thermal (NBRT) index, Tasseled Cap Brightness (TC-B), Digital Elevation Model (DEM), and Principal Component Analysis (PCA). Our findings revealed a strong positive correlation between spatial resolution and classification accuracy. The 10m resolution imagery achieved superior performance (71% overall accuracy, Kappa = 0.66), effectively discriminated fire-affected areas across different age classes (1-3 and 3-5 years post-fire) under varying grazing intensities. The 30m resolution data showed significantly low accuracy (39% overall accuracy, Kappa = 0.34). Higher-resolution imagery substantially reduced salt-and-pepper noise and enhanced visual interpretability. This research confirmed that integrated multi-sensor data processing provides a robust approach for monitoring rangeland dynamics. The methodology offers valuable capabilities for mapping fire-affected vegetation and supports management strategies in extensive, topographically challenging environments where traditional field-based methods are impractical.

Keywords: Fusion, Burned pasture, Gram-Schmidt, Grazing intensity, Classification

Cite this article: Mohammadian, A., Asadi Borojeni, E. & SiahMansour, R., (2026). Assessment of Integrated Landsat-8 and Sentinel-2 Images on Identification and Resolution of the Burned Rangelands (Case Study: Semi-steppe Rangelands in Chahar-Mahal Bakhtiari, Province, Iran), *Journal of Rangeland Science,* 16(3), 278-288. https://doi.org/10.57647/jrs.2026.1603.25

1. Introduction

Fire and overgrazing in rangelands are two of the most pressing threats to natural landscapes, unequivocally shown to degrade rangeland ecosystems and drastically impair their ecological resilience and functionality (Abedini et al., 2022). Therefore, the rangeland monitoring and awareness of the extent of fires, as well as the investigation of grazing management status in the desired rangelands, particularly after the occurrence of such disasters as fire and grazing, are the most essential actions to recognize and manage the rangelands

successfully. On the other hand, mapping large fire-affected areas in rangelands using traditional methods is difficult, particularly when fire zones have complex, sloping topography and are inaccessible due to heterogeneous vegetation. One effective approach is the use of remote sensing techniques and data to map fire-affected areas. In this regard, remote sensing data provide powerful tools that attract the attention of researchers due to various data, including pixel size, time, and large extent. In the present time, assessing and investigating the changes of disasters using satellite images is one of the important branches in the science of natural resources and it is a suitable tool to monitor and control the types of changes in the forest and rangeland ecosystems (Genc and Altunel, 2025). Landsat-8 and Sentinel-2 satellites make free use of satellite imagery possible for researchers. The Landsat-8 satellite is a result of collaboration between NASA and the Geological Society of America and was launched in 2013 (Topaloglu et al., 2016). The Sentinel-2 satellite has been designed by the European Space Agency and has been in Earth's orbit since 2015 (Vafaei et al., 2018). Nowadays, there are different types of remote sensing data provided by a variety of satellites that are used for some applications as detecting vegetation changes. On the other hand, meeting the needs of using remote sensing data given from the Earth's surface is not possible, and it is not sufficient to use one specific method. Therefore, its understanding is more precisely the combination of data that can be more appropriate (Pandit and Bhiwani, 2015). A combination of satellite images is used as the integration of images to produce data with a higher information level from the primary images (Bioresita et al., 2019). Generally, integration methods are categorized into three distinct classes: A) pixel-based methods integrated at the level of physical features, representing the lowest processing tier; B) feature-based integration using characteristics extracted from the data; and C) decision-level methods by decision-makers from diverse resources at the highest processing level (Rangzan et al., 2019; Karimi et al., 2017).

In fact, one of the limitations of the Landsat-8 satellite is that the images can only be taken every 16 days from a specific zone and the images may be damaged because of cloudy weather, meaning they cannot be used and analyzed due to cloud coverage. Landsat-8 data alone are insufficient for comprehensive monitoring of land surface changes, particularly vegetation dynamics (Gao et al., 2015; Atkinson et al., 2012).The Sentinel-2 satellite consists of two polar orbiting satellites, which contribute to the continuity and improvement of the Landsat and Spot satellite missions and provide high quality and reliable data (Celik and Altunel, 2025). The Sentinel-2 satellite bands have the corresponding wavelengths and similar geographic coordinate system to the Landsat-8 satellite. Moreover, the free access to these two satellites' data provides an appropriate opportunity to integrate these two kinds of data.

In a study, Wang et al. (2017) used an advanced Kriging Area to Point approach and integrated the images of two mentioned satellites to increase the spatial precision of images taken by the Landsat-8 satellite from 30 m to 10 m using the above-mentioned approach. They assessed the vegetation changes. The results indicated the improved spatial quality of images and their improved integration performance and potential applied value. In another study, Liu et al. (2022) used the integration method to integrate the images of Landsat-8 and Sentinel-2 satellites in order to enhance the spatial and qualitative resolution. Research results indicated that not only does the integration of images lead to improved classification precision, but it also decreases the impact of cloud interference. Zhang et al. (2023) in a study found that the dynamic monitoring of plant vegetation and agricultural products requires images over short time periods. In fact, there was no integrated remote sensing product with high spatial-temporal resolution that could be used to monitor vegetation changes.The image integration approach has been used to enhance the spatiotemporal resolution of imagery acquired from the Landsat 8 and Sentinel-2 satellites. According to Zhang et al. (2023), time-series curves of vegetation indices derived from the integrated dataset accurately illustrate changes in both vegetation cover and cropping patterns. Since the different algorithms present different results, plenty of methods have been developed to integrate the images in recent decades (Liu et al., 2020). The selection of a suitable method is significantly important with respect to the algorithm efficiency in the image information retention and the image application scope (Kim et al., 2011). Investigating the research results concerning the identification and separation of fire zones by the use of Landsat-8 and Sentinel-2 satellites and the Gram-Schmidt algorithm, it has been reported that this algorithm is of high capability in improving the spatial information of bands and retaining the spectral information (Ao et al., 2020; Rangzan et al., 2019). One of the integration image applications was conducted by Fazeli et al. (2015) as "The Performance of Landuse Classification Algorithms Using Image Integration Techniques. In this research, four methods, including HPF, Gram-Schmidt, DWT, and PC-Sharpened, have been applied to increase the classification precision. Research results indicated that among the mentioned methods, the Gram-Schmidt method has had the most effect on the precision. Syifa et al. (2020) had identified the burned zones using the optimized support vector machine classification method and the Imperialist

10.57647/jrs.2026.1603.25

Competitive Algorithm (ICA), along with the images of Landsat-8 and Sentinel-2 satellites. The burned zones were identified comparatively and then separated to produce acceptable results. Filipponi (2018) developed the BAIS2 index using the visible range bands of Landsat-8 and Sentinel-2 images, which provided suitable results to identify the burned zones in the rangelands in Italy. In another study to extract the range of burned zones, such spectral indices as NDVI, EVI, and NBR of the Landsat-8 satellite were used in a semi-automatic method to give the results with the error percentage of 2-3% (Stroppiana et al., 2012). A review of published studies indicates that most remote sensing research to date has primarily focused on the identification and classification of forested areas. In contrast, studies addressing burned rangelands have generally been conducted in isolation, often without considering the influence of grazing intensity. The present study introduces a novel approach by exploring the potential to discriminate burned rangelands affected by the combined effects of fire and varying grazing intensities through the integration of multispectral satellite imagery. Accordingly, Landsat 8 and Sentinel-2 imagery were integrated to enhance spatial and spectral resolution, improve classification accuracy, and distinguish burned rangelands of different fire ages under various grazing management programs.

2. Materials and methods

2.1. Study area

Chaharmahal and Bakhtiari Province in Iran, with an area of 16,402 km², is located in the southwest of Iran, at a north latitude of 31°09' to 32°48' and an east longitude of 49°28' to 51°25'. It is situated in the center of the Zagros Mountains, Iran. The area of rangelands is 1.04 million ha, involving 3% good rangelands, 37% medium ones and 60% poor ones. The fires occurred in the rangelands in the case study, primarily in the central and northern parts.

2.2. Research Methodology

At first, the fire profile forms in the semi-steppe rangelands in Zagros Mountain were provided through the protection department of Natural Resources and Watershed Management Organization, Tehran, Iran, followed by the information given by the local people and operators, and the desired sites were selected. In this regard, the grazing intensity was determined in the desired regions according to such parameters as the distance from the livestock water supply (Shahriary et al., 2012; Bastin et al., 2003), the access of livestock to rangelands (Tarhouni et al., 2010), and the total number of livestock in the region based on the sensue reported by the Natural Resources Organization and the customary grazing areas for the local operators after determining a list of burned zones and the fire dates based on the available information (Table 1). In general, 27 burned spots were selected in 17 sites according to the fire age (1-3 years and 3-5 years after the fire) and the grazing intensities (heavy and moderate). Then, the desired range of spots was recorded by GPS. In each fire spot, three main plots were selected. The dimensions of the main plots were varied depending on the desired community and the extent of the fire spot. Since the pixel size dimension in the Landsat-8 satellite is 30×30 m. So, according to the satellite images, these sizes were used as the main plots to analyze vegetation traits and field monitoring. Afterwards, within each macro plot, three subplots 4m^2 were investigated along the transect line (Fig 1).

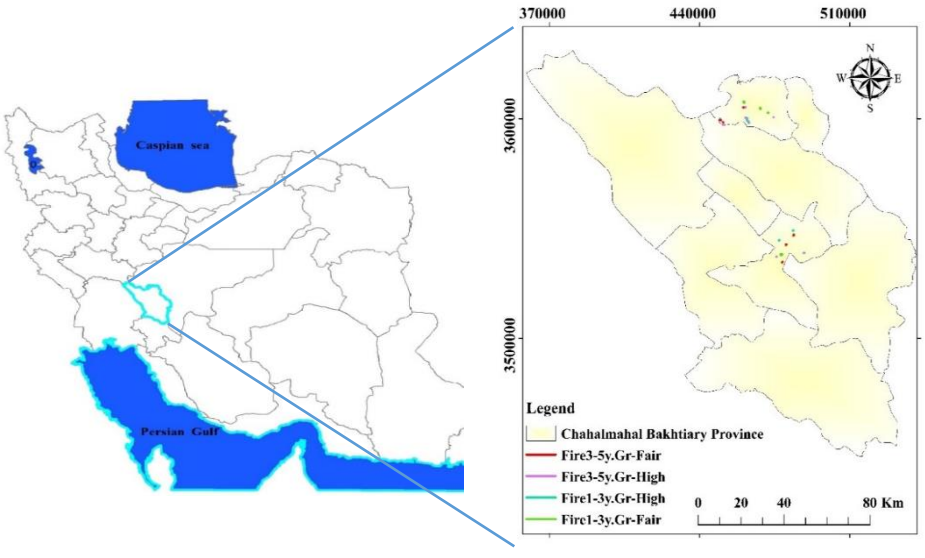

Figure 1. Geographical map of Chaharmahal Bakhtiari province in Iran and fire sites studied in the Semi-steppe rangelands in the right figure

Table 1. A list of vegetation characteristics of selected fire sites in the semi-steppe rangelands of Chaharmahal Bakhtiari province, Iran

Site	No of polygon	Vegetation type	Grazing Intensity#	Fire age year	Longitude X	Latitude Y
Bardeh	4	*Astragalus verus* DC - *Phlomis persica*	High	1-3	462239	3599155
Tang-Gahroo	2	*Astragalus verus* DC. - *Poa bulbosa* L.	High	1-3	488652	3538891
Chaliyab	1	*Astragalus brachycalyx* Fisch – *Gundelia tournefortii* L.	Fair	1-3	460667	3607345
Chezghon1	1	*Daphne mucronata* Royle- *Gundelia tournefortii* L	Fair	1-3	480359	3542488
Kharaji	1	*Astragalus verus* DC. - *Agropyron intermedium* P.Beauv.	High	1-3	483666	3549153
Dastena	1	*Astragalus verus* DC. - *Agropyron intermedium* P.Beauv.	High	1-3	477024	3544649
Sologon1	1	*Astragalus brachycalyx* Fisch – *Agropyron trichophorum* (Link.) Richt	Fair	1-3	478261	3538211
Shahrak	1	*Astragalus verus* DC. - *Bromus tomentellus* Boiss.	Fair	1-3	483558	3547081
Karsanak	2	*Astragalus verus* DC. - *Bromus tomentellus* Boiss.	Fair	1-3	449541	3599246
Larak	2	*Astragalus verus* DC. - *Annual grass.* *Annual forb Poa bulbosa* L.	Fair	1-3	471984	3602743
Amamzadeh	2	*Astragalus verus* DC. - *Agropyron trichophorum* (Link.) Richt	High	3-5	461305	3605072
Bardeh	2	*Astragalus verus DC. - Phlomis persica*	High	3-5	461440	3600342
Ben	1	*Astragalus verus* DC. - *Noaea mucronata Asch. Schneinf.*	High	3-5	474402	3600665
Chezghon2	1	*Astragalus verus* DC. - *Gundelia tournefortii* L	Fair	3-5	480373	3542746
Sologon2	1	*Astragalus brachycalyx* Fisch –*Echinops* ritrodes Bungeau	Fair	3-5	480373	3542736
Shahrak	2	*Astragalus verus* DC. - *Bromus tomentellus* Boiss.	Fair	3-5	483525	3547026
Karsanak	2	*Astragalus verus* DC. - *Bromus tomentellus* Boiss.	Fair	3-5	450961	3598423

High= heavy grazing Fair= moderate grazing

Table 2. Characteristics of satellite images used in the image integration

Satellite	Sensor type	Spatial separation power (m)	bands	Image date	Return period (days)
Landsat-8	Operational Land Imager (OLI)	30	1-7	2017/06/07	16
Landsat-8	Operational Land Imager (OLI)	15	8	2017/06/07	16
Sentinel-2	Multi-Spectral Instrument (MSI)	10	8, 4, 3, 2	2017/05/28	5
Sentinel-2	Multi-Spectral Instrument (MSI)	20	11a, 5, 6, 7, 8	2017/05/28	5

Table 3. Required spectral indices used for fire detection

Complete phrase	Spectral index	Index formula	Reference
Normalized Burn Ratio Thermal	NBRT	$\frac{NIR-(SWIR2*THERMAL1)}{NIR+(SWIR2*THERMAL1)}$	Holden et al., 2005
Tasseled Cap Brightness	TCB	$0{,}303\text{BLUE}+0{,}279\text{GREEN}+0{,}473\text{RED}+0{,}56\text{NIR}+0{,}508\text{SWIR1}+0{,}187\text{SWIR2}$	Baig et al., 2014

SWIR2 = band 7, SWIR1 = band 6, NIR = band 5, RED = band 4, Green = band 3, Blue = band 2, Thermal1= band10

2.3. Integration of landsat-8 and sentinel-2 satellite images

Integrating the satellite images to provide high-level information using the primary images was the main goal of this study. Thus, the Landsat-8 and Sentinel-2 satellite images were integrated to increase the spatial and spectral resolution (Table 2). To minimize the error resulting from the changes in grayscales, the nearest dates of images were considered.

After doing the required corrections on the Landsat-8 satellite images using the pan-sharpening method, the bands 1-7 and the panchromatic 8 band were integrated

with the resolutions of 30 m and 15 m, respectively. Then, a set of 15 m data was developed by the Landsat-8 bands 2-8. To do this, resampling was done on the bands with bigger pixels using the nearest neighbor algorithm to consider the adjacent pixel values for the new ones with the least change in the numerical values of pixels. On the other hand, to integrate the images between the two mentioned satellites, the Gram-Schmidt (GS) algorithm was used. In the GS integration method, a set of vectors was converted to a new set of orthogonal and linearly independent vectors, and a panchromatic band was simulated with low resolution through averaging multispectral bands. Afterwards, a multispectral image was converted as the first band by the GS method, and the components were created according to the number of integrated bands. Then, the panchromatic band with high spatial resolution was replaced by the first GS component. Finally, the reverse GS conversion was done to create the integrated multispectral bands (Ehlers et al., 2010). In this stage, the 30 m bands of Landsat-8 satellite images were enhanced into the ones with the resolution of 10 m using the 10 m bands of Sentinel-2 satellite. After preprocessing the images of Sentinel-2 satellite with a resolution of 10 m and averaging three bands, the panchromatic band (Spatial resolution of 10 m) was simulated with a combination of visible waves. To minimize the movement between the integrated images and the reference image, it is essential to conduct the geometric correction and coordinate operations so that the Root Mean Square Error (RMSE) of several control points between two images is recorded to evaluate the spectral differences between the reference and integrated images (Equation 1).

$$\mathrm{RMSE} = \sqrt{\frac{1}{N}\sum_{i=1}^{N}(X_i - \hat{x_i})^2} \quad (1)$$

xi = Predicted values

$\hat{x_i}$ = observed values

N = total number of samples.

2.4. Determination of classification algorithm and auxiliary data

The selected algorithm was considered the maximum likelihood classification (MLC) in this research. This algorithm is one of the most common classification algorithms in remote sensing studies, which regards the likelihood of putting each pixel in each class while computing the distance between the desired pixel and the average of all classes (Bastarrika et al., 2011). Results achieved in several studies concerning the ability and application of the MLC algorithm have been reported on the burned zones (Kim and Lee, 2021; Ariza et al., 2019; Thariqa et al., 2016). The MLC algorithm in classifying the fire classes along with a set of auxiliary data including the raw pan-sharpening bands (spatial resolution power of 15 m) as a false color combination of Red, Green, Blue (RGB) bands like green, red and infrared red, NBRT and TC-B indices, DEM and PC1, PC2 and PC3 of PCA leading to the increased classification precision of fire classes were used (Mohammadian et al., 2024). The spectral indices in the classification process are presented in Table 3.

2.5. Assessment of classification accuracy

To assess the classification accuracy, the error matrix method was used. The set of first samples was the reference data or test gathered by the field observations. The set of second samples was the pixels labeled by the classifier. To assess and compute the precision of algorithms, a variety of criteria such as the producer precision, user precision, total precision and Kappa coefficients were extracted through the error matrix between the classification images and ground reality map (Fathizad and Tazeh, 2016).

3. Result

3.1. Auxiliary data and false color combination used in the classification process

To classify the images using Landsat-8 satellite data in addition to the raw bands, some auxiliary data were used to achieve the best results and increase the precision in separating the fire zones. The set of auxiliary data used in improving the classification precision of fire classes is presented in Fig 2 and 3. These information layers include the pan-sharpening raw bands (spatial resolution of 15 m) as the false color combination of RGB bands like red, green and blue and NBRT index, as well as TC-B index, DEM and the first three components of PCA index.

3.2. Integration of landsat-8 and sentinel-2 images and classification of fire classes

In the current research, the pan-sharpening and Gram-Schmidt methods were used to integrate the images of the two mentioned satellites. Finally, using three types of data with the spatial resolution of 10, 15, and 30 m and the MLC algorithm, the fire classes were classified. It should be noted that the low RMSE value (0.094) obtained using the Gram–Schmidt algorithm indicates that the fused images show good spatial and spectral compatibility with the reference images. The results of the fire-class classification using the MLC algorithm are presented in Fig 4. Visual comparison and interpretation of the classified images reveal that maps derived from imagery with a 10 m spatial resolution exhibit greater detail and more effectively separate fire classes. In contrast, decreasing the spatial resolution from 10 m to 15 m and 30 m increases the proportion of mixed pixels, resulting in maps characterized by salt-and-pepper noise.

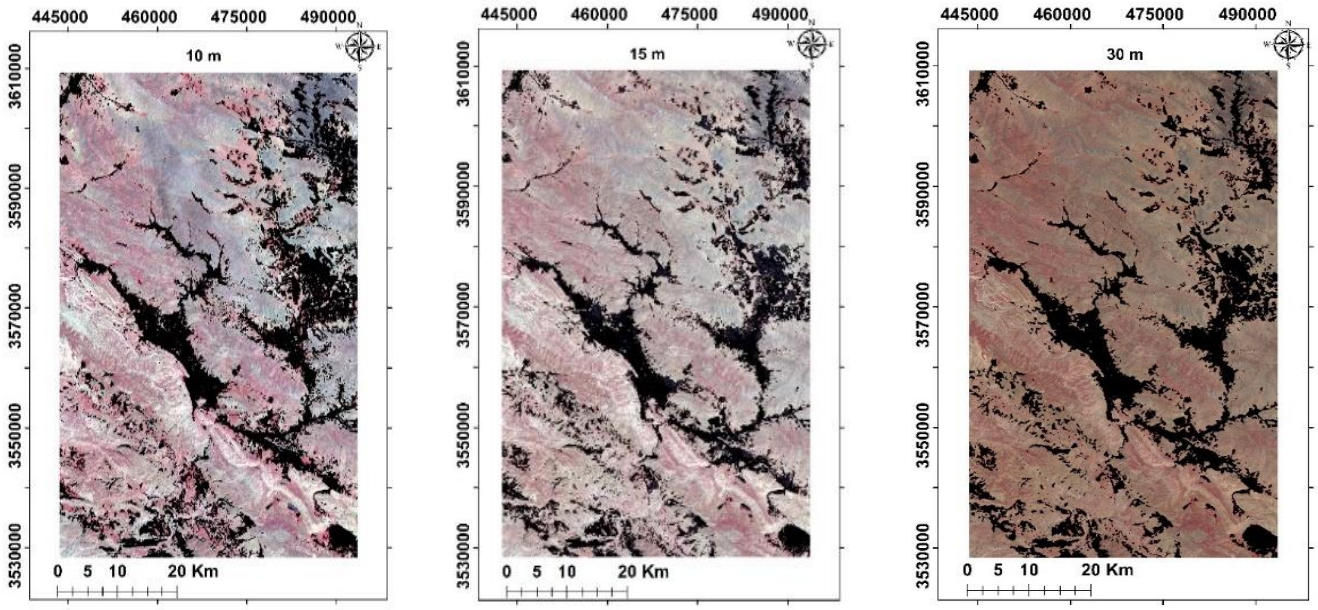

Figure 2. Red, Green, Blue (RGB) map of Landsat-8 satellite images for the 10, 15, and 30 m bands

Table 4. Error matrix of fire classification using Landsat-8 using 15-30 and 10-m bands

Resolution m	Fire age	Grazing intensity	Producer's Accuracy	User's Accuracy	Kappa Coefficient
30 m	Fire (1-3 years)	High	59	61	0.52
		Fair	40	48	0.34
	Fire (3-5 years)	High	34	43	0.30
		Fair	25	31	0.22
	Mean		39%	46%	0.34
15 m	Fire (1-3 years)	High	66	69	0.63
		Fair	53	67	0.50
	Fire (3-5 years)	High	48	54	0.44
		Fair	40	48	0.36
	Mean		51%	60%	0.48
10 m	Fire (1-3 years)	High	88	74	0.80
		Fair	79	80	0.71
	Fire (3-5 years)	High	62	66	0.63
		Fair	53	51	0.49
	Mean		71%	68%	0.66

Results achieved by investigating the classification maps of fire classes using the Landsat-8 satellite images with the resolution of 10, 15, and 30 m indicated that the increased spatial resolution may enhance the precision of classified fire classes. So that the bands with the 10 m resolution of Landsat-8 satellite had the total precision, as 71% and Kappa coefficient, as 0.66, and the Landsat-8 satellite bands with the resolution of 30 m had the lowest precision (39%) and Kappa coefficient (0.34), respectively. The classification accuracy results for fire classes with different fire ages and grazing intensities, derived from bands of varying spatial resolutions, are presented in Table 4. These include the 10 m bands produced by fusing Landsat 8 and Sentinel-2 imagery using the Gram–Schmidt method, the 15 m band obtained from the Landsat 8 panchromatic (PAN) band, and the 30 m bands from Landsat 8.

4. Discussion

In the image integration process, when images are used simultaneously, the result is an integrated image with spatial resolution from the panchromatic image and spectral content from a multispectral image. When images from two different times are used, the aim is to monitor changes within a specific period (Zeng et al., 2010). One of the most commonly applied methods is the Gram-Schmidt conversion for integrating multispectral and panchromatic images.

10.57647/jrs.2026.1603.25

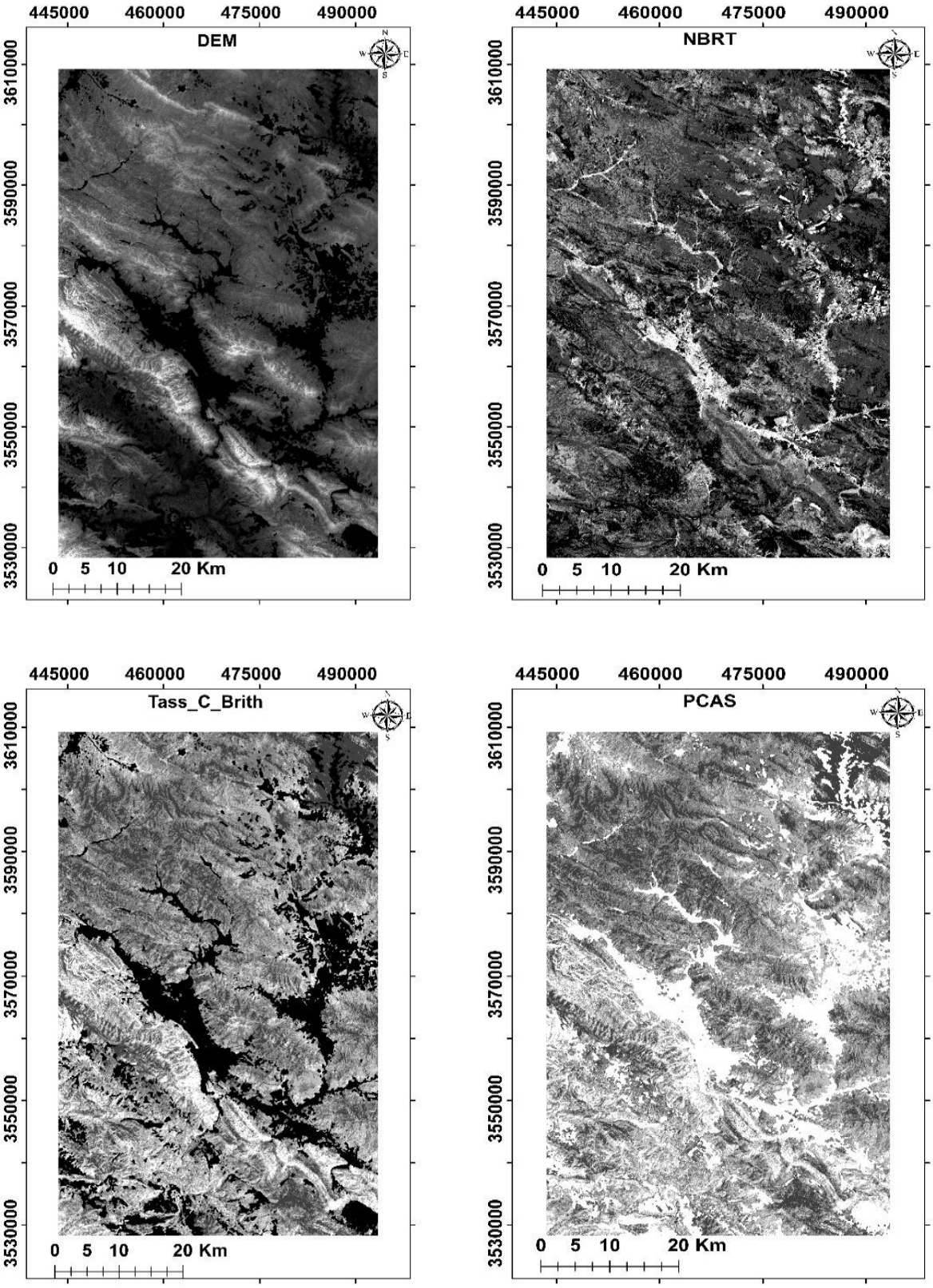

Figure 3. A Set of auxiliary data that increased the classification precision of burned areas during the grazing gradient

10.57647/jrs.2026.1603.25

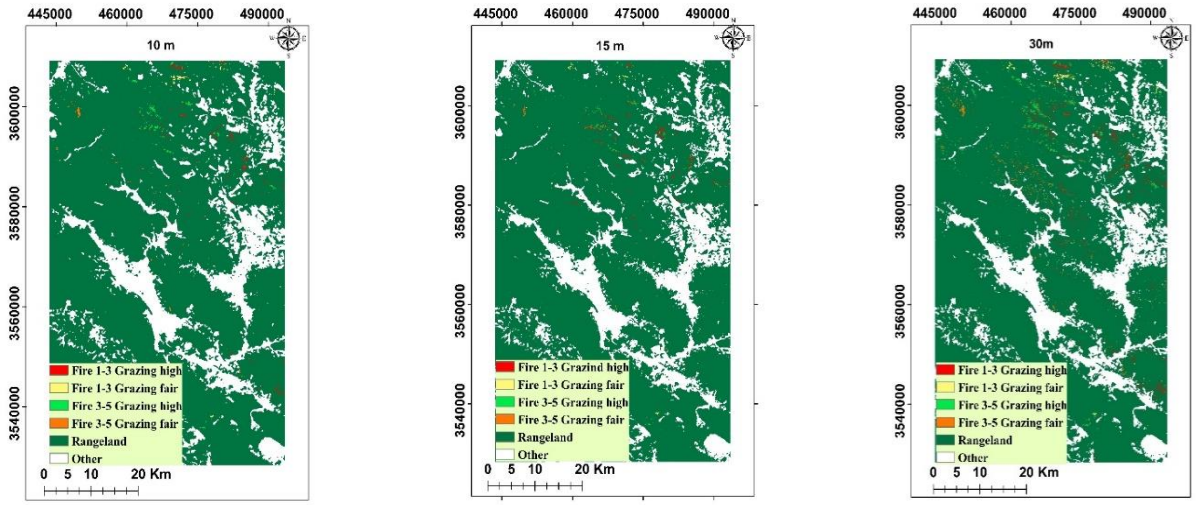

Figure 4. The classification map of fire classes using Landsat-8 10, 15 and 30 m bands

This method has successfully been used to enhance the resolution of multispectral images. The conversion is a mathematical technique for orthogonalizing a linear dependent data set, allowing multispectral images to be expressed in a space where they become independent (Sun et al., 2024).

In this study, to improve classification accuracy in identifying and separating burned areas from surrounding regions, Landsat-8 and Sentinel-2 images were integrated using the Gram-Schmidt method (Sv and Srivasta, 2018). Additionally, to convert images with a spatial resolution of 30 m to 15 m, pan-sharpening techniques and the Landsat-8 panchromatic band were employed. The results showed that increasing the spatial resolution enhances the accuracy of fire classification maps under different grazing management programs. Specifically, the total accuracy and Kappa coefficient of 10 m resolution images increased by 32% compared to 30 m resolution images. These metrics pertain to Landsat-8 images at 10 m resolution processed with the GS algorithm. Findings regarding the integration of Landsat-8 and Sentinel-2 data using the GS algorithm suggested that this method was highly effective at improving spatial details in the bands while preserving spectral information (Rangzan et al., 2019).

The study conducted by Ngadze et al. (2020) on the discrimination and detection of burned rangelands in northwestern Zimbabwe, using Landsat-8 and Sentinel-2 satellite images, demonstrated the superiority of employing 10-meter spatial resolution images obtained from the fusion of Landsat-8 and Sentinel-2 data. This fusion notably enhanced the classification accuracy of small-area burned. Their research findings revealed that although the Landsat-8 OLI sensor has lower spatial and temporal resolution compared to Sentinel-2, it remains useful for detecting burned rangelands and producing burned area maps. Therefore, the fusion of Landsat-8 and Sentinel-2 imagery could significantly enhance the accuracy of burned area. Research results reported by Rafieyan et al. (2022) in terms of desired satellite image capabilities for providing the fire occurrence maps in Arasbaran Forests, Iran, indicated the high potential of the two mentioned satellites and the high ability and facilities of the Google Earth Map system in presenting the remote sensing data. Results showed that the Landsat-8 satellite data were preferred over the Sentinel-2 data because of the thermal band and time series. According to the results, it was proposed to integrate the images of two desired satellites in order to make a large spatial database. Another study was conducted by Baloui and Kabolizadeh (2024) in terms of using different methods of satellite image integration in Ahwaz, Iran. They studied the impact of methods on the classification precision of land use and vegetation and concluded that the GS algorithm using the MLC method, with the Kappa coefficient of 0.84 and total precision of 92.5% showed the best results, which corresponded with the results of the current research. Mahboobi and Azadbakht (2020) investigated the changes in Maharloo Lake using two image integration methods based on the GS algorithm while replacing the main components to increase the classification precision. In addition, they used the MLC and SVM algorithms. Results indicated that the image integration through GS and MLC algorithms could increase the precision significantly, which corresponds with the results in this article. GS and MLC algorithms are useful and reliable tools to investigate and monitor environmental changes. In our study, after extracting the range classes, the

vegetation sub-layers were reclassified to separate the fire classes based on the fire age and grazing intensity. Therefore, considering the similar spectral behavior of fire classes, it was difficult to separate the classes, and consequently, precision decreased, and pixel blending increased. Thus, under the existing conditions, the classification result seems acceptable with a total precision of 66%. Due to the vegetation fires, such spectral changes as loss of chlorophyll, soil erosion, root burning and humidity change happen (Escuin et al., 2008). Taking the fire effects on the detection of vegetation changes in rangelands, spectral indices were used regarding the spectral characteristics of OLI sensing bands of the Landsat-8 satellite and the ratio of spectral-thermal bands in relation to the separation of burned zones from the adjacent regions. Regarding the numerous fires that have occurred in the country's rangelands, the capabilities of Landsat-8 and Sentinel-2 satellite images, along with the benefits of combining these images, can be utilized to enhance the accuracy of identifying and classifying burned rangelands with varying fire ages and different livestock grazing management practices in adjacent areas. Areas with different fire histories and grazing intensities can form distinct plant communities arranged in a mosaic pattern at the landscape scale (Kerby et al., 2007). When fires are accompanied by severe livestock grazing, substantial damage to vegetation structure may occur, followed by changes in the shape and spatial extent of burned patches within rangeland ecosystems. Consequently, accurate identification of burned rangelands is particularly important given their large extent and limited accessibility—especially in mountainous semi-steppe regions—to support effective post-fire management and vegetation recovery planning. So, the integration of desired satellite images can be utilized to identify and separate these rangelands from the adjacent ones successfully. In fact, by increasing the spatial resolution of satellite images and using these images in the classification process using the Maximum Likelihood Classification (MLC) algorithm, it is possible to accurately identify and separate burned rangeland areas with old fires of 1 to 3 years and 3 to 5 years under moderate and high intensity grazing management from their adjacent areas. In the meantime, the GS algorithm can be used as a successful method for merging images and increasing the spatial resolution of Landsat-8 images using Sentinel-2 images.

Actually, the spots with various fire experiences and grazing intensities are capable of creating specific plant communities in a mosaic pattern at the landscape level (Kerby et al., 2007). When the fires are accompanied by severe livestock grazing, they may damage the plant vegetation structure severely followed by changes in the shape and dimensions of fire spots in the range ecosystems, so that the recognition of burned rangelands is considerably important due to the wide extent of rangelands and difficult access to them, especially semi-steppe ones in the mountains to plan and make suitable management decisions after the fire for the revival of plant vegetation. So, the integration of desired satellite images can be utilized to identify and separate these rangelands from the adjacent ones successfully. In fact, by increasing the spatial resolution of satellite images and using these images in the classification process using the maximum likelihood classification (MLC) algorithm, it is possible to accurately identify and separate burned rangeland areas with old fires of 1 to 3 years and 3 to 5 years under moderate and high intensity grazing management from their adjacent areas. In the meantime, the GS algorithm can be used as a successful method for merging images and increasing the spatial resolution of Landsat-8 images using Sentinel-2 images.

5. Conclusion

Rangelands cover about 70% of Iran’s natural resource areas, making it one of the most extensive and important ecosystems. In recent years, the growing number and frequency of burns in semi-steppe rangelands have highlighted the need to identify burned areas accurately. Identifying the precise location and extent of these burned rangelands is crucial for effective post-fire planning and the implementation of management strategies aimed at restoring vegetation cover. Because these rangelands often extend across vast, mountainous, and hard-to-reach areas, mapping and identifying burned zones can be extremely challenging. Remote sensing techniques, however, offer powerful tools for detecting and analyzing fire-affected regions. By integrating satellite imagery from Landsat-8 and Sentinel-2, it is possible to distinguish burned rangelands from surrounding areas more accurately. Enhancing spatial resolution from 30 meters down to 15 or even 10 meters and applying advanced classification methods, such as the Maximum Likelihood Classification (MLC) algorithm, allows for more precise detection and separation of burned rangeland areas with different fire histories (1-3 and 3-5 years post-fire) under varying grazing intensities. When fires occur in rangelands already subjected to heavy grazing, they can cause severe damage to vegetation structure, altering the shape and spatial extent of burned patches across the landscape. Therefore, accurate identification of the extent and boundaries of burned rangelands is essential for developing timely and appropriate post-fire management strategies, as it can strongly influence the effectiveness of rehabilitation efforts and the restoration of vegetation cover in these valuable ecosystems.

10.57647/jrs.2026.1603.25

Acknowledgment

The authors gratefully acknowledge the financial support for this work that was provided by the University.

Authors Contribution
Authors have contributed equally in preparing and writing the manuscript.

Availability of data and materials
The data that support the findings of this study are available on request from the corresponding author.

Conflict of interests
I certify that there is no actual or potential conflict of interest concerning this article.

References

Abedini, M., Shishegaran, M. and Ghale, E., 2022. Monitoring and Estimating the Fire-Affected Areas of the Zagros Mountains Using Landsat Satellite Images. Geography and Environmental Planning, 33(4), 49-62.
DOI: https://doi.org/10.22108/gep.2022.131560.1470

Ao, Z., Sun, Y. and Xin, Q., 2020. Constructing 10-m NDVI time series from Landsat 8 and Sentinel 2 images using convolutional neural networks. IEEE Geoscience and Remote Sensing Letters, 18(8), 1461-1465.
DOI: https://doi.org/10.1109/LGRS.2020.3003322

Ariza, A., Salas Rey, J. and Merino de Miguel, S., 2019. Comparison of maximum likelihood estimators and regression models for burn severity mapping in Mediterranean forests using Landsat TM and ETM+ data. Revista cartográfica, 98, 145-177.
DOI: https://doi.org/10.35424/rcarto.i98.145

Atkinson, P.M., Jeganathan, C., Dash, J. and Atzberger, C., 2012. Inter-comparison of four models for smoothing satellite sensor time-series data to estimate vegetation phenology. Remote sensing of environment, 123, 400-417.
DOI: https://doi.org/10.1016/j.rse.2012.04.001

Baig, M.H.A., Zhang, L., Shuai, T. and Tong, Q., 2014. Derivation of a tasselled cap transformation based on Landsat 8 at-satellite reflectance. Remote Sensing Letters, 5(5), 423-431.
DOI: https://doi.org/10.1080/2150704X.2014.915434

Baloui, F., and Kabolizadeh, M. 2024. Comparative Analysis of Different Image Fusion Methods at the Pixel and Decision Levels on the Accuracy of Land Use and Land Cover Classification. Iranian Journal of Remote Sensing & GIS, 16(3), 1-25. (In Persian).
DOI: 10.48308/gisj.2025.235304.1215

Bastarrika, A., Chuvieco, E. and Martín, M.P., 2011. Mapping burned areas from Landsat TM/ETM+ data with a two-phase algorithm: Balancing omission and commission errors. Remote sensing of Environment, 115(4), 1003-1012.
DOI: https://doi.org/10.1016/j.rse.2010.12.005

Bastin, G., Ludwig, J., Eager, R., Liedloff, A., Andison, R. and Cobiac, M., 2003. Vegetation changes in a semiarid tropical savanna, northern Australia: 1973–2002. The Rangeland Journal, 25(1), 3-19. DOI: https://doi.org/10.1071/RJ03001

Bioresita, F., Puissant, A., Stumpf, A. and Malet, J.P., 2019. Fusion of Sentinel-1 and Sentinel-2 image time series for permanent and temporary surface water mapping. International Journal of Remote Sensing, 40(23), 9026-9049.
DOI: https://doi.org/10.1080/01431161.2019.1624869

Celik, D.A. and Altunel, A.O., 2025. Is dynamic world a contender in global land-cover making race? A swift field assessment from Kastamonu, Türkiye. The Egyptian Journal of Remote Sensing and Space Sciences, 28(2), 205-213.
DOI: https://doi.org/10.1016/j.ejrs.2025.04.002

Ehlers, M., Klonus, S., Johan Åstrand, P. and Rosso, P., 2010. Multi-sensor image fusion for pansharpening in remote sensing. International Journal of Image and Data Fusion, 1(1), 25-45.
DOI: https://doi.org/10.1080/19479830903561985

Escuin, S., Navarro, R. and Fernández, P., 2008. Fire severity assessment by using NBR (Normalized Burn Ratio) and NDVI (Normalized Difference Vegetation Index) derived from LANDSAT TM/ETM images. International Journal of Remote Sensing, 29(4), 1053-1073. DOI: https://doi.org/10.1080/01431160701281072

Fathizad, H. and Tazeh, M., 2016. Assessment of pixel-based classification (ARTMAP fuzzy Neural Networks and Decision Tree) and Object-Oriented methods for land use mapping (Case study: Meymeh, Ilam province). Journal of Arid Biome, 5(2), 69-82. (In Persian).
DOI: https://doi.org/20.1001.1.2008790.1394.5.2.6.4

Fazeli, F.A., Ghazavi, R. and Farzaneh, M.R., 2015. Investigation of landuse classification algorithms using image fusion techniques (Case study: Beheshtabad Sub-basin). Journal of RS and GIS for Natural Resources,6 (1), 91-105. (In Persian).

Filipponi F., 2018, BAIS2: Burned Area Index for Sentinel-2. In: Proceedings of the 2nd International Electronic Conference on Remote Sensing; 22 March–5 April 2018; Online. Basel, Switzerland: MDPI.
DOI: https://doi.org/10.3390/ecrs-2-05177

Gao, F., Hilker, T., Zhu, X., Anderson, M., Masek, J., Wang, P. and Yang, Y., 2015. Fusing Landsat and MODIS data for vegetation monitoring. IEEE Geoscience and Remote Sensing Magazine, 3(3), 47-60.
DOI: https://doi.org/10.1109/MGRS.2015.2434351

Genc, C.O. and Altunel, A.O., 2025. Monitoring the operational changes in surface reflectance after logging, based on popular indices over Sentinel-2, Landsat-8, and ASTER imageries. Environmental Monitoring and Assessment, 197(1), 1-16.
DOI: https://doi.org/10.1007/s10661-024-13526-w

Holden, Z.A., Smith, A.M.S., Morgan, P., Rollins, M.G. and Gessler, P.E., 2005. Evaluation of novel thermally enhanced spectral indices for mapping fire perimeters and comparisons with fire atlas data. International Journal of Remote Sensing, 26(21), 4801-4808.
DOI: https://doi.org/10.1080/01431160500239008

Karimi, D., Akbarizadeh, G., Rangzan, K. and Kabolizadeh, M., 2017. Effective supervised multiple-feature learning for fused radar and optical data classification. IET Radar, Sonar & Navigation, 11(5), 768-777.
DOI: https://doi.org/10.1049/iet-rsn.2016.0346

Kerby, J.D., Fuhlendorf, S.D. and Engle, D.M., 2007. Landscape heterogeneity and fire behavior: scale-dependent feedback between fire and grazing processes. Landscape Ecology, 22, 507-516.

Kim, S. and Lee, S., 2021. Maximum likelihood estimation of probabilistic non-suppression model for OECD NPP electrical fire applying a non-negative continuous distribution. Fire Safety Journal, 122, p.103323.
DOI: https://doi.org/10.1016/j.firesaf.2021.103323

Kim, Y., Eo, Y., Kim, Y. and Kim, Y., 2011. Generalized IHS-Based Satellite Imagery Fusion Using Spectral Response Functions. Etri Journal, 33(4), 497-505.
DOI: https://doi.org/10.4218/etrij.11.1610.0042

Liu, X., Liu, Q. and Wang, Y., 2020. Remote sensing image fusion based on two-stream fusion network. Information Fusion, 55, 1-15.
DOI: https://doi.org/10.1016/j.inffus.2019.07.010

Liu, X., Yang, G., Que, Q., Wang, Q., Zhang, Z. and Huang, L., 2022. How Do Landscape Heterogeneity, Community Structure, and Topographical Factors Contribute to the Plant Diversity of Urban Remnant Vegetation at Different Scales?. International Journal of Environmental Research and Public Health, 19(21), p.14302.
DOI: https://doi.org/10.3390/ijerph192114302

Mahboobi, H. and Azadbakht, M., 2020. Synergy of multi-temporal image fusion and classification methods for detecting changes in Maharlu Lake over five years (2013-2018). Environmental Sciences, 18(1), 203-218.
DOI: https://doi.org/10.29252/envs.18.1.203

Mohammadian, A., Asadi-Broujeni, E. and Siahmansour, R., 2024. Evaluating of multi-spectral remote sensing data in capability to distinguish burned rangelands during grazing gradient (case study: semi-arid rangelands of CHB province, Iran). Iranian Journal of Forest and Range Protection Research, 22(2), 201-221. (In Persian). DOI: https://doi.org/10.22092/ijfrpr.2024.365082.1618

Ngadze, F., Mpakairi, K.S., Kavhu, B., Ndaimani, H. and Maremba, M.S., 2020. Exploring the utility of Sentinel-2 MSI and Landsat 8 OLI in burned area mapping for a heterogenous savannah landscape. PLoS One, 15(5), 1-13.
DOI: https://doi.org/10.1371/journal.pone.0232962

Pandit, V.R. and Bhiwani, R.J., 2015. Image fusion in remote sensing applications: A review. International Journal of Computer Applications, 120(10), 22-32.
DOI: https://doi.org/10.5120/21263-3846

Rafieyan, O., Valizadeh, K.K., Ramazan, M.E. and Moshiri, S., 2022. Comparative evaluation of Landsat8 and Sentinel2 images to prepare a fire occurrence map in Arasbaran.
DOI: https://doi.org/10.30495/jrnr.2022.69827.10260

Rangzan, K., Kabolizadeh, M., Karimi, D. and Zareie, S., 2019. Supervised cross-fusion method: a new triplet approach to fuse thermal, radar, and optical satellite data for land use classification. Environmental monitoring and assessment, 191, 1-12.
DOI: https://doi.org/10.1007/s10661-019-7621-y

Shahriary, E., Palmer, M.W., Tongway, D.J., Azarnivand, H., Jafari, M. and Saravi, M.M., 2012. Plant species composition and soil characteristics around Iranian piospheres. Journal of Arid Environments, 82, 106-114.
DOI: https://doi.org/10.1016/j.jaridenv.2012.02.004

Stroppiana, D., Bordogna, G., Carrara, P., Boschetti, M., Boschetti, L. and Brivio, P.A., 2012. A method for extracting burned areas from Landsat TM/ETM+ images by soft aggregation of multiple Spectral Indices and a region-growing algorithm. ISPRS Journal of Photogrammetry and Remote Sensing, 69, 88-102.
DOI: https://doi.org/10.1016/j.isprsjprs.2012.03.001

Sun, Y., Zhi, X., Jiang, S., Fan, G., Yan, X. and Zhang, W., 2024. Image fusion for the novelty rotating synthetic aperture system based on the vision transformer. Information fusion, 104, p.102163.
DOI: https://doi.org/10.1016/j.inffus.2023.102163

Sv, A.K. and Srivatsa, S.K., 2018. An image fusion technique based on sparse wavelet transform and non-singleton type-2 FNN techniques. TAGA J, 14, 76-86.
DOI: https://doi.org/10.3390/s22187055

Syifa, M., Panahi, M. and Lee, C.W., 2020. Mapping of post-wildfire burned area using a hybrid algorithm and satellite data: The case of the campfire wildfire in California, USA. Remote Sensing, 12(4), p.623.
DOI: https://doi.org/10.3390/rs12040623

Tarhouni, M., Salem, F.B., Belgacem, A.O. and Neffati, M., 2010. Acceptability of plant species along grazing gradients around watering points in Tunisian arid zone. Flora-Morphology, Distribution, Functional Ecology of Plants, 205(7), 454-461.
DOI: https://doi.org/10.1016/j.flora.2009.12.020

Thariqa, P., Sitanggang, I.S. and Syaufina, L., 2016. Comparative analysis of spatial decision tree algorithms for burned area of peatland in rokan hilir riau. TELKOMNIKA (Telecommunication Computing Electronics and Control), 14(2), 684-691.
DOI: http://doi.org/10.12928/telkomnika.v14i2.3540

Topaloglu, R.H., Sertel, E. and Musaoglu, N., 2016. Assessment of classification accuracies of Sentinel-2 and Landsat-8 data for land cover/use mapping. The International archives of the photogrammetry, remote sensing and spatial information sciences, 41, 1055-1059.
DOI: https://doi.org/10.5194/isprs-archives-XLI-B8-1055-2016

Vafaei, S., Soosani, J., Adeli, K., Fadaei, H., Naghavi, H., Pham, T.D. and Tien Bui, D., 2018. Improving accuracy estimation of Forest Aboveground Biomass based on the incorporation of ALOS-2 PALSAR-2 and Sentinel-2A imagery and machine learning: A case study of the Hyrcanian forest area (Iran). Remote Sensing, 10(2), 172.
DOI: http://doi.org/10.3390/rs10020172

Wang, Q., Blackburn, G.A., Onojeghuo, A.O., Dash, J., Zhou, L., Zhang, Y. and Atkinson, P.M., 2017. Fusion of Landsat 8 OLI and Sentinel-2 MSI data. IEEE Transactions on Geoscience and Remote Sensing, 55(7), 3885-3899.
DOI: http://doi.org/10.1109/TGRS.2017.2683444

Zeng, Y., Zhang, J., Van Genderen, J.L. and Zhang, Y., 2010. Image fusion for land cover change detection. International Journal of Image and Data Fusion, 1(2), 193-215.
DOI: https://doi.org/10.1080/19479831003802832

Zhang, H., Zhang, Y., Gao, T., Lan, S., Tong, F. and Li, M., 2023. Landsat 8 and Sentinel-2 Fused Dataset for High Spatial-Temporal Resolution Monitoring of Farmland in China's Diverse Latitudes. Remote Sensing, 15(11), p.2951.
DOI: https://doi.org/10.3390/rs15112951